UDC666.762.9:621.431.73

R & D on Functional Structural Ceramics (Application to Sliding Parts)

Masanori Ueki*1

Abstract:

High hardness, high specific rigidity (Young's modulus/density), low thermal expansion coefficient, and high wear resistance are beneficial properties for the commercialization of structural ceramics. Paying attention to these properties, discussions are made on the application of high strength silicon nitride ceramics to an apex seal, the sliding part of the rotary engine, and on the application of titanium carbide-graphite system composite material to an electroconductive sliding component, as examples of the commercial application of sintered ceramic substrates in a simple plate form which is prepared by the hot-pressing method. The improved friction and wear performance of silicon carbide whisker-reinforced silicon nitride ceramics against the properties of bearing steel are also described as another example of improvement in sliding characteristics, an important requirement for the application of structural ceramics to sliding parts.

1. Introduction

Amid an overheated new material boom about 10 years ago, advanced ceramics were touted to herald the advent of a "second stone age". Now that the ceramics fever has subsided, it will be reasonable to view that advanced ceramics have established a firm position in some applications, but their application to structural parts is still to be pushed forward. This situation is attributable to their drawbacks mainly in thermal shock resistance, and the immaturity of their manufacturing techniques, such as forming techniques, in particular. On the R & D front, an ambitious approach toward simultaneously solving both the product performance and manufacturing technology problems is apparently running short of the set goal in both attempts.

Under the circumstances, Nippon Steel temporarily shelved the ceramics forming technology and focused its R & D efforts on the service performance of advanced ceramics as materials in some of its development projects. The procedure adopted involves producing simple shapes in plate form by the hot pressing process, a uniaxial pressure-assisted sintering process, and machining prototype parts or evaluation specimens from the shapes. Advanced ceramic materials thus produced were finally evaluated by users for specific applications, and the results of evaluation were fed back for further development and improvement. After many such research and development efforts, some of the new advanced ceramics are very highly rated by their intended users and are already in commercial production or are approaching the commercialization phase.

Heat resistance has been traditionally the most coveted functional property of ceramics for service performance in its structural application. As already noted, however, lack in thermal shock resistance has hampered the usage of ceramics in structural applications, and low toughness has made it difficult to use them in applications subject to mechanical shock. The properties of ceramics that can be immediately put to practical use, on the other hand, are hardness, specific stiffness (Young's modulus/density), low thermal expansion, and wear resistance. Among them, the low thermal expansion is a right fit property for preci-

*1 Technical Development Bureau

sion equipment parts used at near or under room temperature. The combination of low thermal expansion with hardness, stiffness and wear resistance is expected to open up new applications to components of various electronic and semiconductor device fabrication equipment. It should be kept in mind, however, that the part size increase and formability of the components will become important issues in such applications.

Structural ceramics find such a field of application where only their material properties count without regard to the part size increase or the formability problem. Among such applications, this report describes the commercial application of silicon nitride ceramics to the apex seals of rotary engines and also the development of titanium carbide-graphite system composites applied as electroconductive sliding parts. The addition of silicon carbide whiskers to a silicon nitride ceramics is also discussed as a typical method to improve the sliding performance as against a bearing steel.

2. Development of High-Strength Silicon Nitride Ceramics and Its Application to Apex Seals of Rotary Engine (RE)[1,2]

2.1 Rotary engine and apex seals

The rotary engine has a rotor that is equivalent to the piston of a reciprocating engine and rotates as implied by its name. It is relatively free from the power loss and vibration attendant on the reciprocative motion of the piston and valves in the engine, is structurally simple and lightweight, and rotates with much smoothness and less noise.

The construction of the rotary engine is schematically illustrated in **Fig. 1(a)**. The triangular rotor rotates within the trochoidal case (rotor housing) in the shape of a cocoon. A mixture of gasoline and air is introduced through the intake port, compressed, and electrically ignited. The pressure of the burning and expanding gas produces power. Three types of gas seals are used on the rotary engine. The apex seals located at the three apexes of the rotor prevent the escape of the exploding gas and compressed gasoline-air mixture. The side seals prevent the gas leakage through the sides of the rotor. The corner seals are arranged at the joining points of the apex and side seals[3].

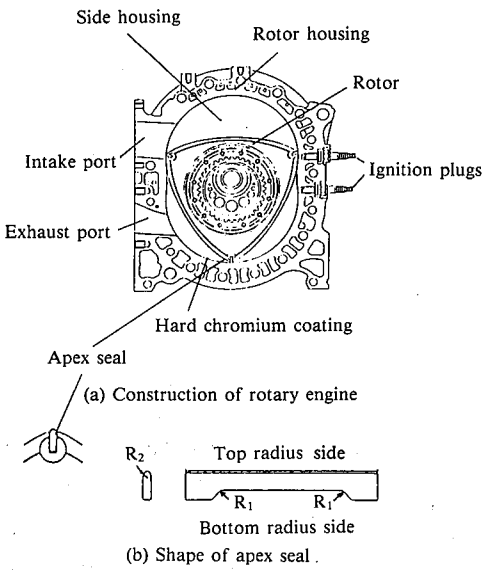

Fig. 1 Construction of rotary engine and shape of apex seal

The apex seal is shaped as shown in **Fig. 1(b)**, and is a critical component similar to the piston ring of the reciprocating engine. The apex seals slide at high speed on the inside surface of the rotor housing and are pressed against the inside surface by the expanding gas pressure during combustion, the inertial force due to rotation, and the spring force. The properties required of the apex seal material are therefore mechanical strength against these forces and sliding performance against the hard chromium coating applied to the inside surface of the rotor housing.

2.2 Development of high-strength silicon nitride ceramics

Table 1 lists the mechanical properties of several hot-pressed silicon nitride ceramics under development at Nippon Steel. When attention is focused on the flexural strength columns, it is evident that room-temperature flexural strength and high-temperature flexural strength are difficult to coexist in silicon nitride ceramics to which various sintering agents are added. That is, the silicon nitride ceramics A in **Table 1** boasts an extremely high room-temperature flexural strength of about 1,450 MPa, but suffers a great loss of flexural strength at elevated temperatures of 1,200°C and above. The ceramics B through E have relatively low room-temperature flexural strengths of 1,000 to 1,200 MPa, but their loss of flexural strength is smaller at elevated temperatures. The ceramics E, in particular, retains a high flexural strength of about 800 MPa even at 1,400°C. In view of these differences, it must be noted that silicon nitride ceramics is a multiple-phase material composed of silicon nitride crystal grains and intergranular phases binding the grains.

It was the room-temperature flexural strength that the user specified as the first requirement to be met when silicon nitride was to be applied as a material for the apex seals. Given the operating environment of the apex seals, elevated-temperature properties appear rather important, but no evidence is found that the entire apex seals are exposed to a high temperature of 1,000°C or above during service. As requested by the user, Nippon Steel submitted the material A in **Table 1** in competition with other materials supplied from ceramic manufacturers. The material A with an extremely high room-temperature flexural strength won the competition and was adopted as the material for the apex seals to be used in the rotary engines of racing cars.

The microstructures of the material A observed by transmission electron microscope are shown as bright-field and dark-field images in **Photo 1(a)** and **(b)**[4], respectively. As evident from the images, the material A consists only of considerably aciculated ß-Si_3N_4 crystal grains and intergranular glass phases. The acicular grains are oriented normal to the hot press axis (perpendicu-

Table 1 Mechanical properties of various hot-pressed silicon nitride ceramics

Material symbol	Composition (agent)	Density (%TD)	Flexural strength (MPa)				Hardness (Hv)	Fracture toughness K_{IC} (MPa$\sqrt{m}$)
			Room temp.	1000°C	1200°C	1400°C		
A	YMC	99.1	1450	970	300	Deform	1513	6.7
B	YZ	99.9	1000	1030	920	560	1602	7.2
C	YC	99.6	1080	950	1080	640	1706	6.9
D	YCZ	99.2	990	880	820	220	1437	7.9
E	YH	99.6	1220	1040	850	770	1733	8.5

TD: Theoretical density, Flexural strength: As per JIS R 1601 and R 1064
K_{IC}: As per JIS R 1067

Photo 1 Transmission electron micrographs of hot-pressed silicon nitride ceramics (material A) (a) bright-field image; and (b) dark-field image. (Since their electron diffraction image shows a halo pattern, intergranular phases are amorphous.)

lar to the page), and the mechanical properties are clearly anisotropic[5].

2.3 Application to Le Mans 24-hour Grand Prix race cars — Recovery and analysis of used apex seals —

The Mazda 767 B powered by a rotary engine with apex seals of the silicon nitride ceramics made by Nippon Steel made a debut in the Suzuka Japan Race in April 1989[6]. Three Mazda 767 B racing cars participated in the Le Mans 24-hour Grand Prix in June of the same year, and all ran their full distance. Still another Mazda 767 B car ran the full distance in the 1990 Le Mans 24-hour Grand Prix race. These results validated the high durability and reliability of the ceramic-made apex seals.

Apex seals were recovered from the rotary engine of a Mazda 26 B racing car that had run a distance of about 5,300 km in the Le Mans 24-hour Grand Prix race in June 1989. When the recovered apex seals were examined with the naked eye, a magnifying glass, and an optical microscope, wear was found at four portions on the leading surface (surface A) and at two portions on the opposite surface (surface B), as shown in **Fig. 2**. These wear portions can be classified according to the cause of wear as follows: 1) wear due to sliding against the inside surface of the rotor housing (true sliding wear) (portion a in **Fig. 2**); 2) wear due to friction against the corner slot (portions b, c, and d in **Fig. 2**); and 3) wear of the bottom corner radius due to friction against the plate spring.

When the wear portions were examined in more detail, it was found that abrasive wear tracks due to sliding became conspicuous from the edge of seals toward the center. Particularly at the center, two-step sliding abrasive wear tracks were observed. The formation of the two steps may be attributed to the fact that the angle at which each apex seal contacts the trochoidal rotor housing is slightly different between the upper and lower parts of the trochoidal curve. However, the top radius of the apex seal was worn only very slightly, and appeared mirror finished, except for some portions where wear tracks were clearly noticeable.

True sliding wear that does severe damage to the apex seals was limited to the so-called "shoulder chipping wear" that takes place at the center of the top radius. This damage is considered to occur as follows. When the apex seals pass the intake port and exhaust port at the center in the depth direction normal to the page (thickness direction of the rotor housing) in **Fig. 1(a)**, its center (same as the diameter of each port) loses the support by the top radius and projects into the port by elastic deformation. As the rotation of the rotor goes on, the projecting portion of the apex seal comes to clash against the port edge. The resultant impact causes marked wear at the center of the top radius on the leading surface.

As noted above, wear is caused in the two-step form because the apex seal passes the intake and exhaust ports at different angles of contact. **Photo 2** gives an optical macrograph of the typical shoulder chipping wear taken from above the top radius. When the wear portions were observed by scanning electron microscopy, a metallic lustrous adhesion was observed as shown in the portions 1 and 2 in **Photo 3(a)**. The two portions are enlarged in **Photo 3(b)** and **(c)**, where fine cracks arising from the adhesion are visible to a considerable degree. Examination by energy-dispersive X-ray spectroscopy (EDS) of the portions A and B in **Photo 3(c)** indicated that the adhesive wear debris is composed mainly of chromium removed from the inside surface of the rotor housing.

Typical examples of ceramic chipping observed in the shoulder chipping wear portions are shown in **Photo 4**. As clear from **Photo 4**, the local chipping of the apex seal is caused by the adhesion of chromium. The chromium adhesion involves chromium-to-chromium friction with increased frictional coefficient and resistance.

On the other hand, as the rotor turns and slides, the adhesive wear interface is repeatedly heated and cooled locally. The difference in the coefficient of thermal expansion between the chromium coating and the silicon nitride ceramics imposes tensile stress on the surface of the silicon nitride ceramics that is lower

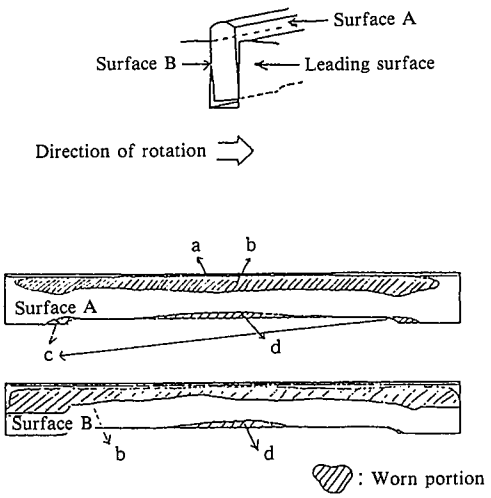

Fig. 2 Wear of apex seal (sketch)

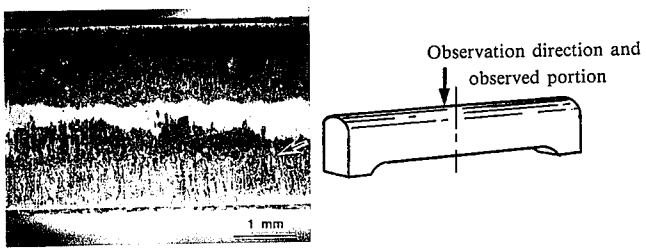

Photo 2 Optical macrograph of shoulder chipping wear portion in top radius of apex seal (step indicated by an arrow)

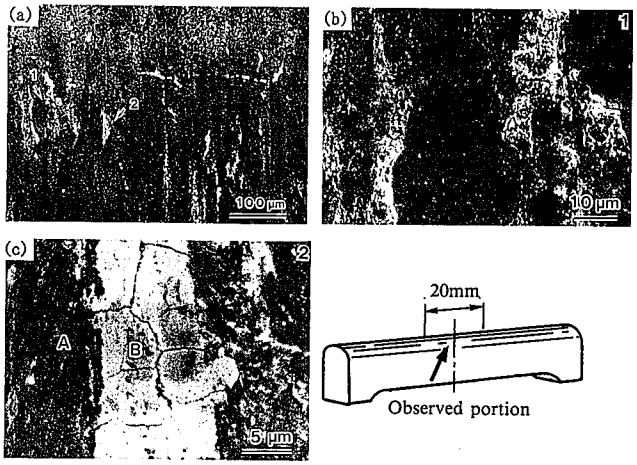

Photo 3 Scanning electron micrographs of top radius of apex seal. Portions 1 and 2 in micrograph (a) of relatively low magnification are shown in micrographs (b) and (c) of high magnification, respectively.

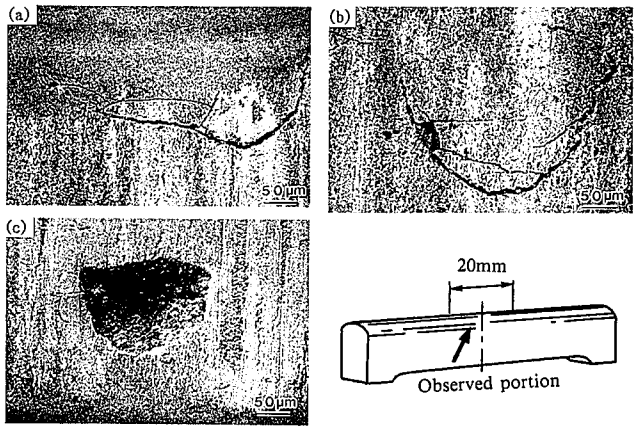

Photo 4 Scanning electron micrographs of wear portion in top radius of apex seal. Chromium adhesion and crack occurrence at the wear portion are shown.

in the coefficient of thermal expansion. This tensile stress causes the chipping (wear) of the silicon nitride ceramics in the form of peeling the surface layer of the apex seal. The mechanism at work here is that the harder ceramics (Si_3N_4 with Hv = 1,500) and the softer metal (hard chromium coating with Hv = 1,000) slide against each other, when wear is caused on the harder side.

The apex seal surface layer is damaged to a severe degree as already noted, but the damage appears to be extremely localized. Investigation was made of the extent of the damage suffered by the silicon nitride ceramics material in the engine that had run a distance of several thousand kilometers. In this investigation, a bending fracture test was carried out on the used apex seals, and the test results of their failure load were compared with those of unused apex seals to determine the gravity of damages. From the test results it was found that the fracture loads of the used apex seals were higher than those of the unused apex seals, which result makes it reasonable to think that the silicon nitride ceramics in the bulk form was little damaged when used as the apex seals. Many of the above-mentioned fine cracks were observed in the shoulder portions close to the side surface and grew at angles close to parallel along the surface, indicating little or no adverse effect on them.

The early fear that the bulk of the apex seal ceramics might be degraded by thermal damage when exposed to the high-temperature environment in the racing car engine was thus proved to be unfounded. It now seems unnecessary even to apply apex seals made of silicon nitride ceramics that has the intergranular phases crystallized and features superior elevated-temperature strength.

2.4 Development of new material on the basis of results of practical use

The investigation and analysis of the used apex seals recovered from the racing car engine as described above indicated the need for a further improvement in sliding characteristics. In other words, the demand mounted for a ceramic material that is relatively immune to the adhesion of the hard chromium coating. Close observation revealed that the adhesion was pronounced at the grain boundaries composed mainly of oxide and was caused little in the silicon nitride grains themselves. On the basis of these experimental findings, a plan was made to reduce the use of oxide-base sintering aids.

Under a conventional method, the reduction in the amount of sintering agent directly translates into the reduction in strength for sintered silicon nitride substrates. Therefore, we adopted a method using a premixed powder of sintering agent prepared by the sol-gel method[7], and a new material with approximately the same room-temperature strength as the conventional material was successfully produced by using only about a half of the sintering agent amount, as shown in **Fig. 3**. The wear characteristics of the new material as against the hard chromium coating were examined. When the comparison was made of compositions having practically the same strength (sintering agent additions of 8 to 12 wt%), it was found that the smaller the sintering agent addition, the smaller is the amount of wear.

3. Development of Titanium Carbide-Graphite System Composite Material and Its Application to Current Conductive Parts

3.1 Material development guideline

Titanium carbide (TiC) is a unique ceramic material that has high melting point and high hardness characteristic of covalent-bond materials, and electric conductivity comparable to that of metals[8]. Sintered TiC itself is low in toughness[9], however, and its applications are limited to the main component of the material

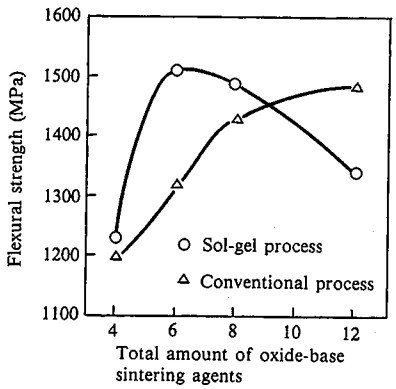

Fig. 3 Effect of the amount of oxide-base sintering agent on room-temperature flexural strength of hot-pressed silicon nitride ceramics

for cermet tools, dispersant in ceramics-based composites and thin or thick coating films. To improve the properties of TiC and expand its field of application as structural ceramics, attempts have been made to combine TiC with various second phases[8,10,11]. Among such composites, particularly worth noting here are TiC-graphite system composites with graphite dispersed as second phase. The TiC-graphite system composites are not only superior in strength, toughness[11] and machinability, but are expected to demonstrate a new self-lubricating function when used as sliding parts[12].

Nippon Steel has been developing this material system jointly with a user for practical application as current conductive parts. In this work, Nippon Steel is in charge of material development and the user company undertakes material evaluation. Described here are the mechanical properties of the TiC-graphite system composites and the effect of the combination of TiC with graphite on improving the sliding characteristics of the TiC-graphite system composites against copper (Cu) in dry air as evaluated by the pin-on-disk test method.

3.2 Evaluation of sliding characteristics[13]

Fig. 4[14] shows the test scheme and test conditions of the sliding section in the pin-on-disk wear testing machine used. The pin is fixed, and the disk is rotated at a constant speed, being driven by a dc motor. The test load is applied to the pin set up at the point of action of a lever from outside of the test chamber through a vacuum bellows. The frictional force and the load can be detected by a strain gauge attached near the pin support of the lever. Copper (OFHC Cu) was used as the pin specimen, and a TiC-graphite system composite was used as the disk specimen. The test method is discussed in detail in Reference 14. The coefficient of friction and specific wear of the TiC-graphite system composites were evaluated in comparison with those of representative structural ceramics against copper. **Table 2** summarizes the compositions and mechanical properties of the TiC-graphite system composites used.

3.3 Coefficient of friction and specific wear

The change with time in the coefficient of friction during the pin-on-disk sliding test is shown for each test material in **Fig. 5**[12]. In **Fig. 5(a)**, the coefficient of friction for TiC begins to change about 400 s after the start of the test, and its average value

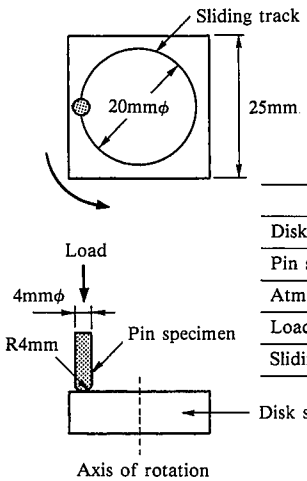

Test conditions	
Disk specimen	TiC, TiC-graphite composite
Pin specimen	Cu (OFHC)
Atmosphere	Dry air
Load	8.3 N
Sliding speed	62.8 mm/s

Fig. 4 Schematic illustration of pin-on-disk test method and test conditions

Table 2 Compositions and mechanical properties of TiC and TiC-graphite system composites

		TiC	TiC-graphite composite		
Carbon	wt%	0	10	15	20
	vol%	0	19.6	27.9	35.4
Density	g/cm^3	4.85	4.35	4.09	3.81
	%TD	98.2	98.6	97.6	95.6
Flexural strength (MPa)		376	520	373	272
K_{IC} (MPam$^{1/2}$)		3.4	3.6	4.2	3.5
Vickers hardness (Hv)		2200	1450	700	250

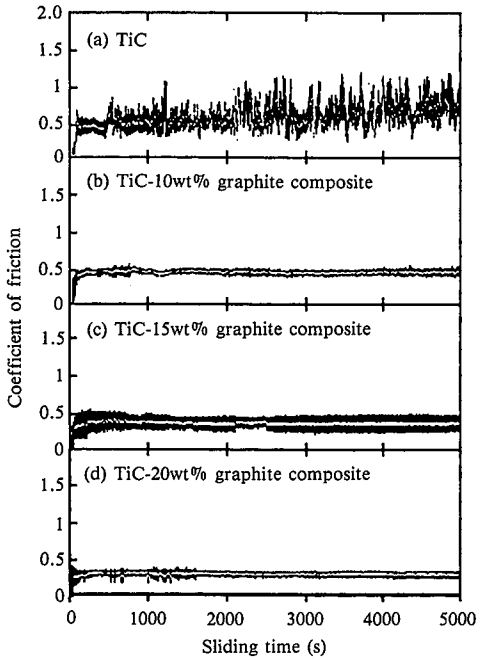

Fig. 5 Change with time in friction coefficient of TiC-graphite system composites sliding against copper in dry air

continues to increase even after 500 s. With regards the TiC-graphite system composites shown in **Figs. 5(b)** through **(d)**, in contrast, the variation of friction coefficient is smaller on the whole, and their average friction coefficient decreases with increasing amount of graphite addition.

Next, these results of evaluation were compared with those of such other structural ceramics as silicon nitride (Si_3N_4; Toshiba Tungalloy FX950, sintered under normal pressure and HIPed), silicon carbide (SiC; Ibiden SC850, sintered under normal pressure), alumina (Al_2O_3; Toshiba Ceramics ADS-11, sintered under normal pressure), and zirconia (ZrO_2; Tosoh PSZ powder, sintered under normal pressure). The sliding characteristics of these materials against copper in dry air were compared with those of the TiC-graphite system composites. The following specific wear rate of the pin specimen was used as an index:

$$\text{Specific wear rate (mm}^2\text{/N)} = \frac{\text{Wear (mg)/Density (mg/mm}^3\text{)}}{\text{Sliding distance (mm)} \times \text{Load (N)}}$$

The results of evaluation are shown in **Fig. 6**[13]. The specific wear rate of TiC is of the order of 10^{-8} mm^2/N, approximate-

ly the same as that of Al_2O_3 and lower than that of the other three ceramics, but the addition of graphite can reduce it to the order of 10^{-9} mm^2/N.

Photo 5[12] shows the surfaces of the TiC-20 wt% graphite composite as observed by high-resolution scanning electron microscopy. In **Photo 5(a)**, graphite and TiC appear dark and bright, respectively. Graphite edges are thinned to appear bright, and laminar graphites are dispersed as if to cover up TiC grains. In the higher-magnification micrograph of **Photo 5(b)**, delamination of graphites are observed, and some fine laminar graphites are shown adhering to the surface of TiC grains. These microstructures attest to the aforementioned finding that the TiC-graphite system composites have self-lubricating characteristics and exhibit superior sliding characteristics.

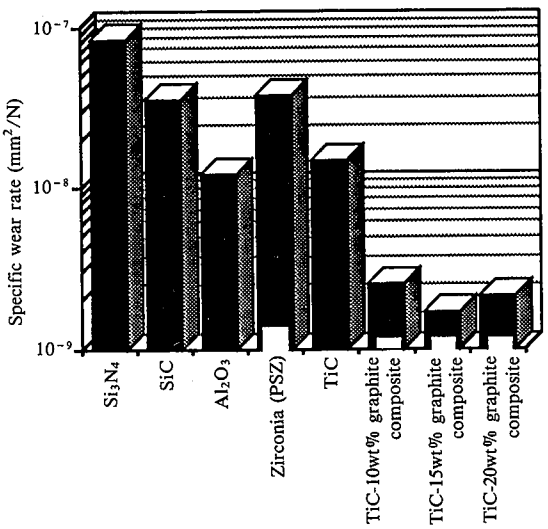

Fig. 6 Specific wear comparison of copper pins slid against TiC-graphite composites and various other ceramics

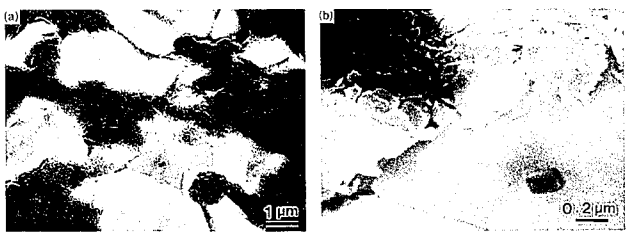

Photo 5 High-resolution scanning electron micrographs of polished surfaces of TiC-20wt% graphite composite

4. Improvement in Sliding Characteristics of Silicon Nitride Ceramics Against Bearing Steel by Adding Silicon Carbide Whiskers[15]

4.1 Material compatibility in sliding pairs

Attention is paid here to the problem of adhesive wear, the governing wear mechanism for many sliding pairs. The amount of wear can be reduced by increasing the strength of the materials comprising the sliding pair, or by decreasing the adhesive force between the materials, so as to cause a shear fracture at their contact interface. In other words, adhesive wear is influenced by two factors, namely, the individual material strength of the sliding pair and their compatibility[16,17]. Compatibility is of particular importance. However good their mechanical properties may be, the materials comprising the sliding pair will suffer a larger amount of wear if they develop a chemical reaction or interfacial adhesion between them. When they are compatible with each other, on the other hand, they exhibit good sliding characteristics and suffer little wear even if they are not high in strength or hardness. Among sliding pairs of good compatibility are silver/iron (Ag/Fe)[17] and above-mentioned copper/alumina (Cu/Al_2O_3)[18].

Attempts have been made to clarify the factors that govern sliding compatibility between materials. One explanation uses a phase diagram for sliding between pure metals[17], and another cites the oxidation activity of a pure metal in its wear against alumina (Al_2O_3)[18]. Regrettably, however, none of these efforts has gone beyond providing solutions to specific problems. Presented here are the results of investigation conducted on the sliding characteristics of silicon carbide whisker-reinforced silicon nitride ceramics against bearing steel with attention focused on sliding material compatibility.

4.2 Test conditions and materials

The test apparatus used was the pin-on-disk wear testing machine described earlier. The test conditions are given in **Table 3**, and the chemical compositions, mechanical properties and manufacturing processes of the test materials are as listed in **Table 4**. The test materials were three types of composites consisting of hot-pressed silicon nitride (Si_3N_4) to which yttria (Y_2O_3) and alumina (Al_2O_3) were added as sintering agents, Si_3N_4 as the matrix to which 10 to 30wt% silicon carbide (SiC) whiskers were added, and commercial silicon carbide (SiC) designated by Ibiden

Table 3 Sliding test conditions for SiC whisker-reinforced Si_3N_4 ceramic against bearing steel

Sliding speed (mm/s)	100
Load (N)	28
Sliding distance (m)	1000
Test atmosphere	Dry air

Table 4 Compositions and mechanical properties of ceramic specimens

Matrix	SiC whisker (wt%)	Sintering process	Density (g/cm^3)	Flexural strength (MPa)	Fracture toughness ($MPam^{1/2}$)	Hardness (Hv)
Si_3N_4	0	Hot pressing	3.24	1029	5.5	1540
	10		3.24	1025	6.7	1820
	20		3.22	989	6.9	1990
	30		3.23	940	7.7	1790
SiC (Ibiden SC850)	0	Sintering under normal pressure	3.11	850	2.5	2400

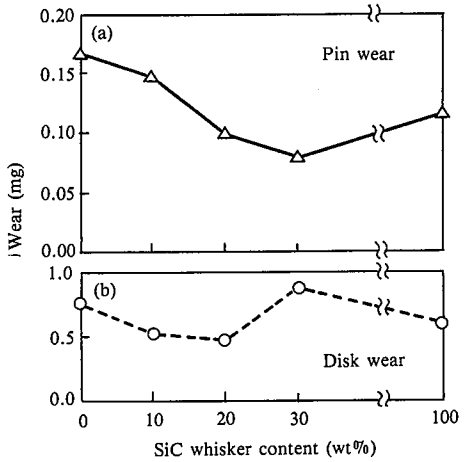

Fig. 7 Effect of SiC whisker content in silicon nitride on sliding wear of silicon nitride system ceramic pin and bearing steel disk

SC850 for comparison. JIS SUJ2 bearing steel was used as mating material. It was heat treated under the same conditions as for actual use, and its Vickers hardness was Hv 870. With the sliding pairs of these materials, the bearing steel was tested as the pin specimen, and each ceramics was tested as the disk specimen.

4.3 Effect of silicon carbide whiskers on sliding characteristics

Figs. 7(a) and **(b)** respectively show the wear of the ceramic pin specimen and the bearing steel disk specimen as a function of the amount of silicon carbide (SiC) whisker contained in the ceramic pin. The wear of the bearing steel disk specimen shown in **Fig. 7(b)** does not clearly indicate the effect of SiC whisker addition, but the wear of the ceramic pin specimen evidently decreases with increasing amount of SiC whisker addition.

When the sliding surfaces of the ceramic pins are observed by scanning electron microscopy, the transfer of the wear from the bearing steel is evident. The wear of the bearing steel transferred to the pin specimen is in large pieces when the SiC whisker addition is low, and is in smaller and fewer pieces when the SiC whisker addition is high. The Si_3N_4 matrix with SiC whiskers composited was roughened on its sliding surface, but revealed little adhesion. It was also observed that the wear of the bearing steel containing iron (Fe) as the main composition is preferentially transferred to the silicon nitride ceramic matrix while avoiding the silicon carbide whiskers.

According to the results of observation on the sliding surfaces and the wear test results shown in **Fig. 7**, silicon carbide is well compatible with steel causing scarcely any adhesion to the steel, whereas silicon nitride is less compatible with steel causing appreciable adherence to the steel. This is probably because the addition of silicon carbide whiskers makes the silicon carbide partially exposed to the sliding surface to prevent its adhesion to the steel, resulting in improving its compatibility with steel and reducing wear on the whole.

The above experimental results tell that, when a wear-resistant ceramics is to be developed with the object of applying it to a component sliding against a metal, not only strength, toughness, hardness and other mechanical properties but also compatibility with the mating material must be taken into consideration.

5. Conclusions

Apex seals and current conductive components have been described as examples of those for which the possibility of enlargement or shaping other than machining need not be considered, paying attention only to hardness, specific rigidity (Young's modulus/density), low thermal expansion and wear resistance.

The slackening demand for advanced ceramics is due not only to poor performances low thermal shock resistance, in particular and immature manufacturing techniques as previously mentioned, but also to the lack of good coordination between material manufacturers and users. It is said that the application of new materials to mechanical and structural components calls for drastic changes in conventional design concepts. Regrettably, however, there are few cases in which such changes are implemented under good coordination between the manufacturer and user what is most wanted in new materials is an accumulation of actual service performance record, which is causing the users to hesitate to use them. The good coordination between the user and the manufacturer reported here is an extremely rare case. In this case, used apex seals were recovered from the user, and investigated and analyzed from the standpoint of a material manufacturer. The value of the findings obtained was immeasurable.

6. Acknowledgments

The author would like to express gratitude to Mazda Motor Corporation for its permission to present this report within the scope of the secrecy agreement concluded in connection with the joint development project.

References

1) Ueki, M.: Shinsozai ("New Materials" in Japanese). 3 (9), 68 (1992)
2) Yamaguchi, Y.: Automotive Eng. 98, 93 (1990)
3) RE Rotary Engine. Mazda Technical Information, Nov. 1986, p. 23
4) Mishima, M. et al.: Proc. 3rd Autumn Meeting, Ceramic Society of Japan, 1990, p. 512-513
5) Sato, Y. et al.: Proc. 3rd Autumn Meeting, Ceramic Society of Japan, 1990, p. 514-515
6) Nikkei Mechanical, July 24, 1989, p. 71
7) Sato, Y. et al.: Mat. Res. Soc. Symp. Proc. Vol. 287. 1993, p. 429-434
8) Ueki, M. et al.: ISIJ Int. 32 (8), 943 (1992)
9) Kamiya, A. et al.: J. Ceram. Soc. Japan. 98, 1146 (1990)
10) Endo, H. et al.: J. Mater. Sci. 26, 3769 (1991)
11) Ueno, K. et al.: J. Ceram. Soc. Japan. 97, 507 (1989)
12) Ono, T. et al.: Materials System. 11, 57 (1992)
13) Ono, T. et al.: Proc. JAST Tribology Conf. Morioka, October 1992, p. 405
14) Fukuda, K. et al.: Proc. JAST Tribology Conf. Tokyo, May 1990, p. 325
15) Fukuda, K. et al.: Proc. 11th Meeting on the High-Temp. Mat. Hakone, December 1992, Ceramic Society of Japan
16) Rabinowicz, E.: ASLE Trans. 14, 198 (1971)
17) Sasada, T. et al.: Proc. 20th Jap. Congr. Mat. Res. 1977, p. 99
18) Enomoto, A. et al.: Proc. 5th Int. Congr. on Tribology (EUROTRIB '89), 1, 1989, p. 111